

MEAN LOAD EFFECT ON FATIGUE OF WELDED JOINTS USING STRUCTURAL STRESS AND FRACTURE MECHANICS APPROACH

JONG-SUNG KIM^{1*}, CHEOL KIM¹, TAE-EUN JIN¹ and P. DONG²

¹Korea Power Engineering Company

360-9 Mabuk-dong, Guseong-Gu, Yongin-si, Gyeonggi-do, 449-713, Korea

²Center for Welded Structures Research, Battelle Memorial Institute

King Avenue, Columbus, Ohio, OH43201, USA

*Corresponding author. E-mail : kimjs@kopec.co.kr

Received January 9, 2005

Accepted for Publication April 3, 2006

In order to ensure the structural integrity of nuclear welded structures during design life, the fatigue life has to be evaluated by fatigue analysis procedures presented in technical codes such as ASME B&PV Code Section III. However, existing fatigue analysis procedures do not explicitly consider the presence of welded joints. A new fatigue analysis procedure based on a structural stress/fracture mechanics approach has been recently developed in order to reduce conservatism by erasing uncertainty in the analysis procedure. A recent review of fatigue crack growth data under various mean loading conditions using the structural stress/fracture mechanics approach, does not consider the mean loading effect, revealed some significant discrepancies in fatigue crack growth curves according to the mean loading conditions. In this paper, we propose the use of the stress intensity factor range ΔK characterized with loading ratio R effects in terms of the structural stress. We demonstrate the effectiveness in characterizing fatigue crack growth and S-N behavior using the well-known data. It was identified that the S-N data under high mean loading could be consolidated in a master S-N curve for welded joints.

KEYWORDS : Welded Joint, S-N Curve, Structural Stress, Mean Loading Effect, Fatigue Crack Growth, Stress Intensity Factor

1. INTRODUCTION

It has been reported that almost all fatigue cracks along pressure boundaries are initiated at welded joints in nuclear power plant components and structures. Therefore, in order to ensure the structural integrity of nuclear welded structures during design life, the fatigue life has to be evaluated by fatigue analysis procedures presented in technical codes such as ASME Boiler and Pressure Vessel Code Section III [1]. However, the existing analysis procedure does not explicitly consider the presence of welded joints. Furthermore, a consistent characterization of stress concentration effects due to local discontinuities on welded joints cannot be readily achieved with a peak stress intensity approach in the fatigue analysis procedure, because the peak stress intensities on welded joints with localized stress gradients are dependent on mesh sizes/types. Therefore, in order to ensure the reliability of analysis results via this procedure, either a more detailed numerical analysis for mesh sensitivity of peak stress intensity is performed or the equivalent linearized stresses from numerical analysis are multiplied by a theoretical stress concentration factor (SCF). The

former is a time-consuming, inefficient approach. For the latter, multiplication of the SCF can ensure the reliability of the analysis results as a result of conservatism. However, this conservatism can cause fundamental problems at the design and life extension stage, because the need to extend the design life and consider the light water reactor environmental effect has recently increased.

As a result, various fatigue analysis procedures have recently been developed in order to reduce the conservatism by erasing the uncertainty of analysis results [2-4]. In particular, Kim, et al.[4,5] developed a new fatigue analysis procedure based on the structural stress and fracture mechanics approach that incorporates mesh-insensitive characteristics and provides a single master S-N curve for weld joints. However, a recent review of fatigue crack growth data [6] under various mean loading conditions using the structural stress and fracture mechanics approach [4], which does not consider the mean loading effect, identified some significant discrepancies in the fatigue crack growth curves according to the mean loading conditions. These discrepancies can be attributed to the mean loading effect, especially according to high mean loading conditions with high loading ratio.

In the present paper, we propose the stress intensity factor range ΔK characterized with loading ratio R effects in terms of the structural stress. We demonstrate the effectiveness in characterizing fatigue crack growth and S-N behavior using the well-known data. The S-N data under high mean loading are consolidated in a master S-N curve for welded joints.

2. STRUCTURAL STRESS AND FRACTURE MECHANICS APPROACH

2.1 Structural Stress

As shown in Fig. 1(a), a typical through-thickness stress distribution at the notch root such as a weld toe exhibits a monotonic through-thickness distribution with the peak stress occurring at the weld toe. It should be noted that in a typical finite element based stress analysis, the stress values within some distance from the notch root such as the weld toe can change significantly as different element sizes or element types are used in the finite element model; this is referred to as mesh-size sensitivity in the literature [7,8]. The corresponding statically equivalent structural stress distribution is illustrated in Fig. 1, in the form of a membrane component σ_m and bending component σ_b , consistent with the elementary structural mechanics definition:

$$\sigma_s^t = \sigma_m^t + \sigma_b^t \quad (1)$$

The super script t denotes the definition of the structural stress with respect to ligament length t in Fig. 1(a) from the notch root.

The normal structural stress σ_s is defined at a location of interest such as Section A-A at the weld toe in Fig. 2 with a plate thickness t . A second reference plane can be defined along Section B-B in Fig. 2, along which both local normal and shear stresses can be directly obtained from the finite elements solution. The distance δ represents the distance between Section A-A and B-B (in local x direction) at the notch root. For convenience, a row of elements with same length of δ can be used in the finite element model. By imposing equilibrium conditions between Sections A-A and B-B, the structural stress components σ_m and σ_b must satisfy eqs. (2) and (3), if there is no loading between Section A-A and B-B:

$$\sigma_m = \frac{1}{t} \int_0^t \sigma_x(y) dy \quad (2)$$

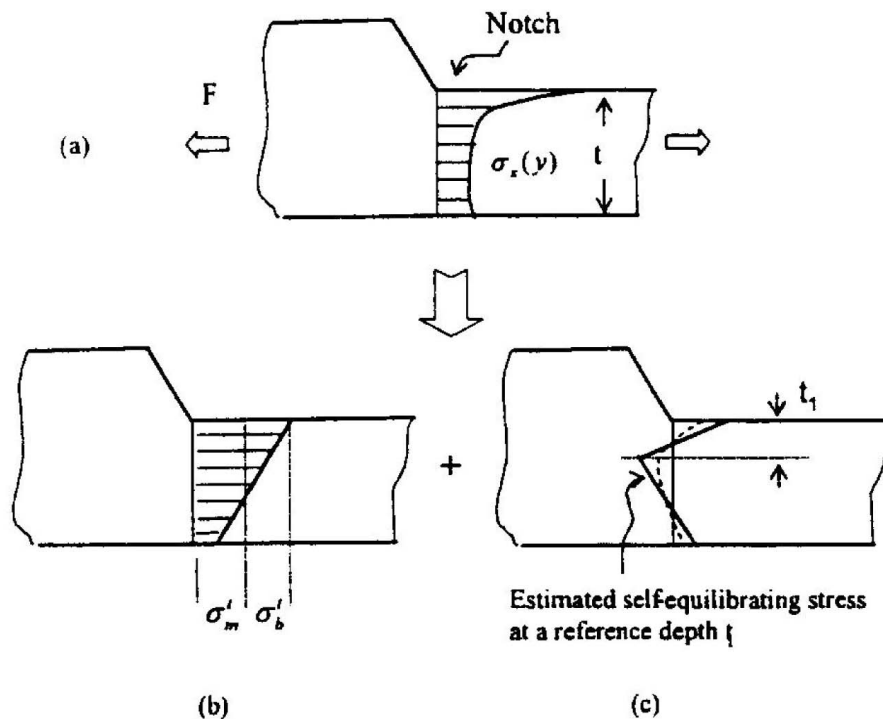


Fig. 1. Through-thickness Structural Stresses Definition: (a) Local Stress from FE Model at a Notch (b) Equilibrium Equivalent Structural Stress (c) Approximation of Self-equilibrating Stresses (Notch Stress) with Respect to a Reference Depth t_l

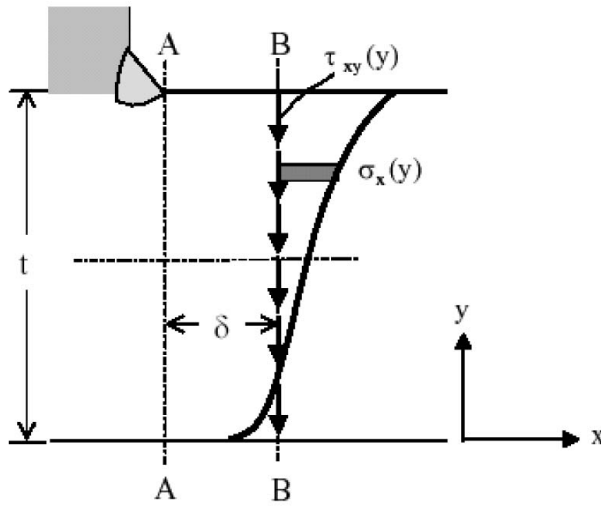


Fig. 2. Structural Stresses Calculation Procedure for Through-Thickness Fatigue Crack

$$\sigma_m \frac{t^2}{2} + \sigma_b \frac{t^2}{6} = \int_0^t \sigma_x(y) y dy + \delta \int_0^t \tau_{xy}(y) dy \quad (3)$$

Eq. (2) represents the force equilibrium in the x direction per unit length in the third direction, evaluated along Section B-B, and eq. (3) represents the moment equilibrium with respect to Section A-A at $y=0$. The second integral term on the right-hand side in eq. (3) represents the transverse shear force as an important component of the structural stress definition. In theory, the mesh-insensitivity of the structural stresses calculated can be assured if the stress states at two planes (Section A-A and B-B) can be related to each other in an equilibrium sense. Since the stresses along Section A-A are influenced by the singularity at the notch root, the structural stress components σ_m and σ_b at the weld toe line (Section A-A) are calculated by performing the integrals in eqs. (2) and (3) along Section B-B.

2.2 Stress Intensity Factor Estimation

The stress intensity factor K_n represents only the through-thickness structural stress combination to the stress intensity factor, as described by eq. (4) for a single edge cracked specimen.

$$K_n = K_{nm} + K_{nb} = \sqrt{t} \left[\sigma_m^t f_m \left(\frac{a}{t} \right) + \sigma_b^t f_b \left(\frac{a}{t} \right) \right] \quad (4)$$

$f_m(a/t)$ and $f_b(a/t)$ in eq. (4) are dimensionless functions of the relative crack size a/t for the membrane and bending components of the structural stress, given in a handbook such as [9]:

$$\begin{aligned} f_m \left(\frac{a}{t} \right) &= \left[0.752 + 2.02 \left(\frac{a}{t} \right) \right. \\ &\quad \left. + 0.37 \left(1 - \sin \frac{\pi a}{2t} \right)^3 \right] \sqrt{\frac{2 \tan \frac{\pi a}{2t}}{\cos \frac{\pi a}{2t}}} \\ f_b \left(\frac{a}{t} \right) &= \left[0.923 \right. \\ &\quad \left. + 0.199 \left(1 - \sin \frac{\pi a}{2t} \right)^4 \right] \sqrt{\frac{2 \tan \frac{\pi a}{2t}}{\cos \frac{\pi a}{2t}}} \end{aligned} \quad (5)$$

As discussed earlier, σ_m and σ_b signify structural stress components that are defined with respect to the entire thickness. Once the structural stresses are available, the stress intensity factor can be readily calculated from eq. (4)

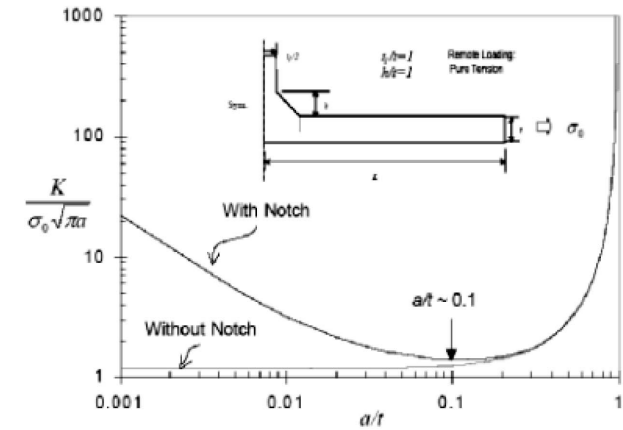
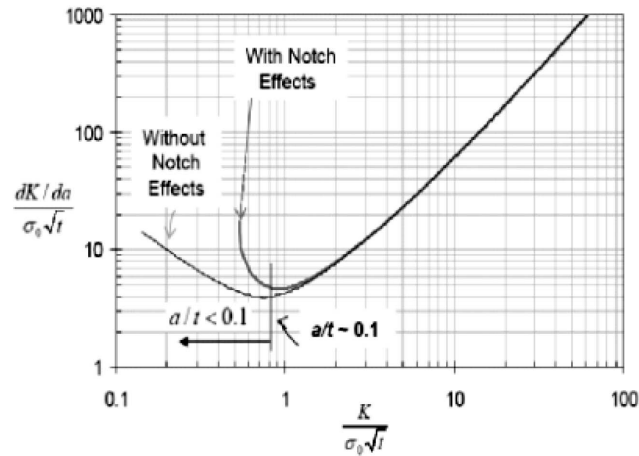
2.3 Fatigue Crack Growth Estimation

The notch-induced stress intensity behaviors can be conveniently characterized by defining the notch-induced stress intensity magnification factor as follows:

$$M_{kn} = \frac{K_{notch}(\text{with local notch effects})}{K_n(\text{based on } \sigma_m^t \text{ and } \sigma_b^t)} \quad (6)$$

In eq. (6), M_{kn} reflects notch stress concentration effects represented by the self-equilibrating part of the actual stress state. The term K_n represents only the through-thickness structural stress contributions to the stress intensity factor. Global stress concentration effects have already been taken into account in K_n . K_{notch} represents the total stress intensity factor due to both the structural stress and the local notch stress effects.

In order to make use of the structural stress based K solutions for fatigue correlation of welded joints, a proper crack growth model needs to be identified. In accordance with previous studies[10,11] for notched fracture mechanics specimens, it is recognized that there are some significant discrepancies in the slope and exponent of the conventional Paris's law between short crack and long crack growth regions; some of the discrepancies can be attributed to the

(a) K versus a/t - T joint

(b) Derivative K versus K

Fig. 3. Stress Intensity Factor Changes as a Function of Crack Size a/t for a T-joint Under Remote Tension

so-called short crack “anomalous growth” effect. In this paper, the anomalous crack growth is explained by demonstrating how such a short crack at a notch can significantly alter the stress intensity behaviors in a continuum mechanics context. As shown in Fig. 3, the notch stress intensity factor solutions K_{notch} demonstrate that non-monotonic K as a function of crack size can develop near a notch tip, if a sharp notch is considered. Furthermore, the elevated K in terms of M_{Kn} diminishes at a relative crack size of approximately $a/t \approx 0.1$. It can then be postulated that the short crack growth process can be characterized by the two distinct

stages of K behavior as a crack propagates from $a/t \leq 0.1$ to $a/t > 0.1$. Also, it can be argued that two stages of stress intensity factor solutions in the form of the notch-stress dominated $\Delta K_{a/t \leq 0.1}$ and far-field stress dominated $\Delta K_{a/t > 0.1}$ can be separated so as to characterize the full range crack growth behavior from $0 < a/t \leq 0.1$ (small crack) to $0.1 < a/t \leq 1$ (long crack). Here, the term ΔK refers to the stress intensity factor range corresponding to the remote stress range. It then follows that:

$$da/dN = C[f_1(\Delta K_{a/t \leq 0.1}) \times f_2(\Delta K_{a/t > 0.1})] \quad (7)$$

Utilizing the definition of the stress intensity magnification factor M_{Kn} in dimensionless form and assuming power-law forms for both $f_1(\Delta K_{a/t \leq 0.1})$ and $f_2(\Delta K_{a/t > 0.1})$, eq. (7) can be re-written as:

$$da/dN = C(M_{Kn})^n (\Delta K_n)^m \quad (8)$$

The terms M_{Kn} and K_n have been discussed in eq. (6). The exponents n and m are determined based on crack growth data covering both typical short crack and long crack regions.

2.4 Equivalent Structural Stress

The fatigue cycle to final failure can be expressed as follows:

$$N = \int_{a \rightarrow 0}^{a=a_f} \frac{da}{C(M_{Kn})^n (\Delta K)^m} \quad (9)$$

The integral in eq. (9) can be written in a relative crack length form as follows:

$$\begin{aligned} N &= \int_{a_i/t \rightarrow 0}^{a/t=1} \frac{td(a/t)}{C(M_{Kn})^n (\Delta K)^m} \\ &= \frac{1}{C} \cdot t^{1-m} \cdot (\Delta \sigma_s)^{-m} \cdot I(r) \end{aligned} \quad (10)$$

where $I(r)$ is a dimensionless function of $r(\sigma_b/\sigma_s)$ after the following integration under a given m :

$$I(r) = \int_{a_i/t \rightarrow 0}^{a/t=1} \frac{d(a/t)}{(M_{kn})^n [f_m(a/t) - r\{f_m(a/t) - f_b(a/t)\}]} \quad (11)$$

Then, eq. (10) can be expressed in terms of N once the dimensionless $I(r)$ function is known:

$$\Delta\sigma_s = C \cdot t^{-\frac{1}{m}} \cdot t^{\frac{2-m}{2m}} \cdot I(r)^{\frac{1}{m}} \cdot N^{-\frac{1}{m}} \quad (12)$$

Eq. (12) describes the structural stress based S-N curves ($\Delta\sigma_s - N$) as a function of thickness effects and bending ratio. If eq. (12) provides a good representation of the fatigue behavior of welded joints, an equivalent structural stress parameter can be defined by normalizing the structural stress range $\Delta\sigma$ with two variables expressed in terms of t and r :

$$\Delta S_s = \frac{\Delta\sigma_s}{t^{\frac{2-m}{2m}} \cdot I(r)^{\frac{1}{m}}} = C \cdot t^{-\frac{1}{m}} \cdot N^{-\frac{1}{m}} \quad (13)$$

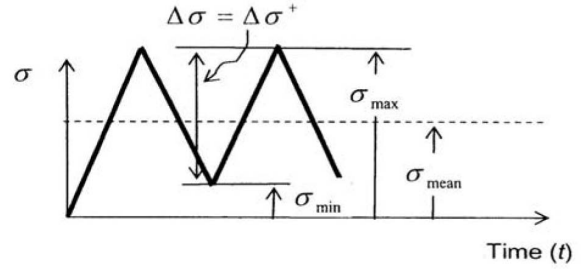
3. FATIGUE ANALYSIS PROCEDURE CONSIDERING HIGH MEAN LOADING

3.1 Fatigue Crack Growth Model

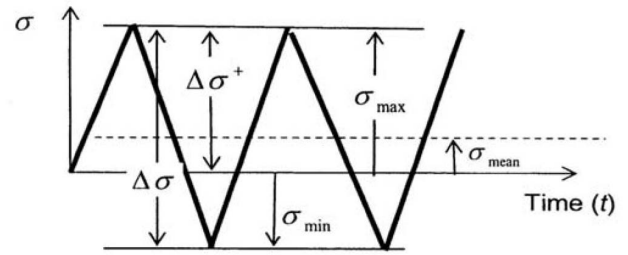
There are various empirical ways to modify the conventional Paris law in eq. (8) for treating the R ratio effects. Recently, the ΔK^* parameter has been gained increasing popularity in the fatigue research community [6,7]. It is defined as:

$$\Delta K^* = \sqrt{\Delta K^+ K_{\max}} \quad (14)$$

ΔK^* refers to the positive range of the stress intensity factor K corresponding to $\Delta\sigma$ in Fig. 4 and K_{\max} corresponding to σ_{\max} . As shown in Fig. 4, two situations need to be considered, depending upon whether the loading ratio ($R = \sigma_{\min}/\sigma_{\max}$) is positive or negative.



(a) $\sigma_{\min} \geq 0$



(b) $\sigma_{\min} < 0$

Fig. 4. Stress Range and Stress Ratio Definition in Cyclic Loading

3.1.1 Positive Stress Ratio

For $\sigma_{\min} \geq 0$, Fig. 4 shows that $\Delta\sigma = \Delta\sigma^+$ and $\sigma_{\max} = \Delta\sigma/(1-R)$. Again, for an edge crack according to eq. (4), it can be shown that:

$$\Delta K^+ = \Delta\sigma_s^+ \sqrt{t} [f_m - r(f_m - f_b)] \quad (15)$$

$$K_{\max} = \frac{\Delta\sigma_s}{1-R} \sqrt{t} [f_m - r(f_m - f_b)] \quad (16)$$

Substituting ΔK^+ and K_{\max} in the above eq. (14), the following is obtained:

$$\Delta K^* = \frac{\Delta\sigma_s}{\sqrt{1-R}} \sqrt{t} [f_m - r(f_m - f_b)] \quad (17)$$

Note that σ_s represents the structural stress calculated with respect to t . In view of the fatigue crack growth model in eq. (14), the loading ratio R effects on the stress intensity factor range, as described in eq. (17), can be included:

$$\frac{da}{dN} \propto \left(\frac{M_{kn}}{\sqrt{1-R}} \right)^n (\Delta K_n)^m \quad (18)$$

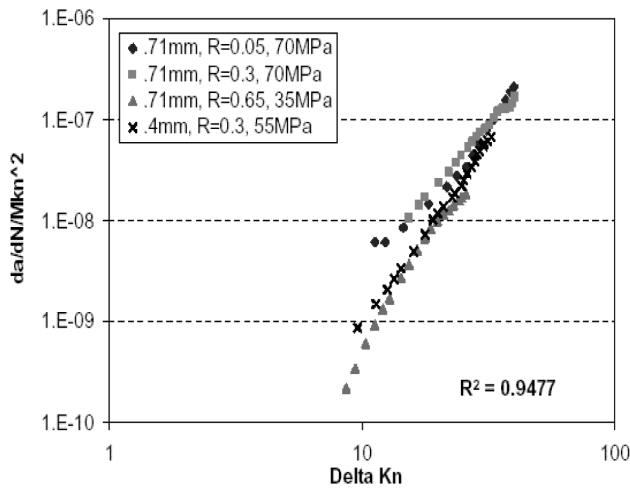


Fig. 5. Fatigue Crack Growth Data Without R Ratio Effects

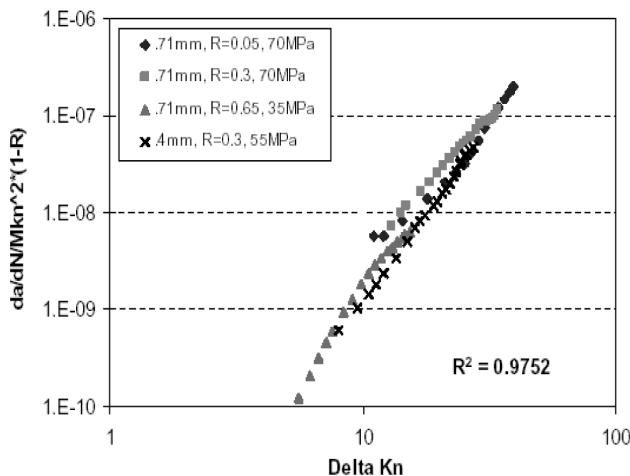


Fig. 6. Consolidated Results of Fatigue Crack Growth with Loading Ratio R Effects

In order to validate the fatigue crack growth model, as described in eq. (18), a subset of experimental data with different R ratio by Shin and Smith [6], who evaluated the effect of notch plasticity and crack closure on fatigue crack growth, was re-analyzed using eq. (18). The results were then compared with those obtained using eq. (8). Fig. 5 shows the fatigue crack growth data from Shin and Smith calculated using eq. (8). The regression correlation parameter R^2 for the four sets of the data is noticeably improved ($R^2=0.98$ versus $R^2=0.95$) when eq. (18) is used, as shown in Fig. 6. The exponent n is determined as 2 in order to consolidate the crack growth data by Shin and Smith [6], as shown in Figs. 5 and 6.

With eq. (18), the equivalent structural stress parameter in eq. (13) becomes:

$$\Delta S_s = \frac{\Delta \sigma_s}{(1-R)^{\frac{1}{m}} \cdot t^{\frac{2-m}{2m}} \cdot I(r)^{\frac{1}{m}}} \quad (19)$$

3.1.2 Negative Stress Ratio

If $\sigma_{min} < 0$, it can be seen from Fig. 4 that $\Delta \sigma_s^+ = \Delta \sigma_s / (1-R)$ and $\sigma_{max} = \Delta \sigma_s / (1-R)$. Eq. (15) thus becomes:

$$\Delta K^+ = \frac{\Delta \sigma_s}{1-R} \sqrt{t} [f_m - r(f_m - f_b)] \quad (20)$$

Identically with the positive stress ratio case, the fatigue crack growth model becomes:

$$\frac{da}{dN} \propto \left(\frac{M_{kn}}{1-R} \right)^n (\Delta K_n)^m \quad (21)$$

Comparing eq. (18) with eq. (21), the loading ratio R effects on crack growth rate are much stronger if R is negative than if R is positive. The equivalent structural stress parameter incorporating the negative R -ratio can be expressed as:

$$\Delta S_s = \frac{\Delta \sigma_s}{(1-R)^{\frac{2}{m}} \cdot t^{\frac{2-m}{2m}} \cdot I(r)^{\frac{1}{m}}} \quad (22)$$

3.2 Consolidation of S-N Data

The fatigue tests employed a very high ratio as one of the five testing conditions, as shown in Fig. 7. In condition

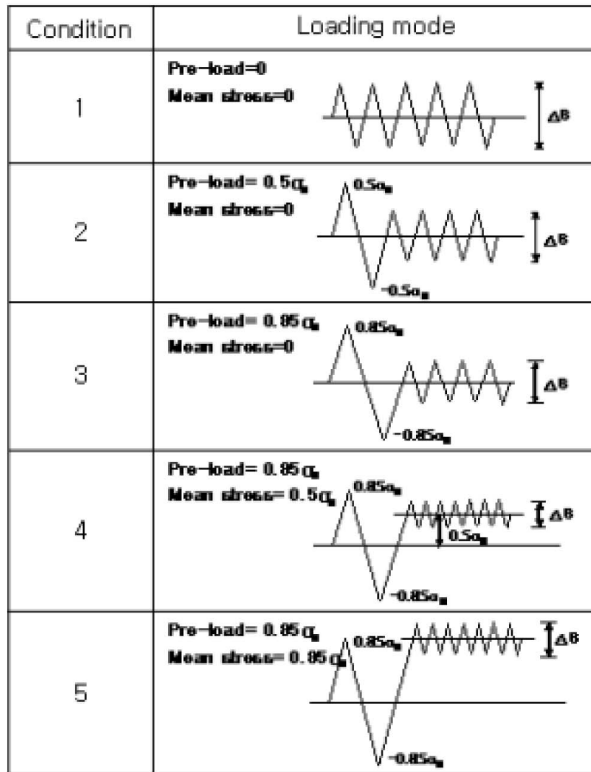


Fig. 7. Conditions of Pre-loading and Mean Load for Tests

5, the mean nominal stress was 85% yield strength of the base material. The nominal stress based S-N data is first converted to a plot in terms of the equivalent structural stress range versus N according to eq. (13) without considering R effects, as shown in Fig. 8(a). In Fig. 8(a), S-N data under condition 4 and condition 5 are significantly lower than those under the other three conditions.

Upon use of the equivalent structural stress range parameter according to eq. (19), Fig. 8(b) shows a significant improvement over Fig. 8(a). It is important to note that if $R=0$ (e.g., conditions 1-3 in Fig. 7), eq. (19) becomes identical to the original equivalent structural stress range definition in eq. (13). Therefore, all discussions regarding the data remain valid even if eq. (18) is proven more effective in the instance that a strong R effect is proven to be important. This is intended to demonstrate the applicability of the present structural stress/fracture mechanics approach to consider high mean loading effects. As additional data in this category are collected in the future, the need to consider the loading ratio effects can be further investigated.

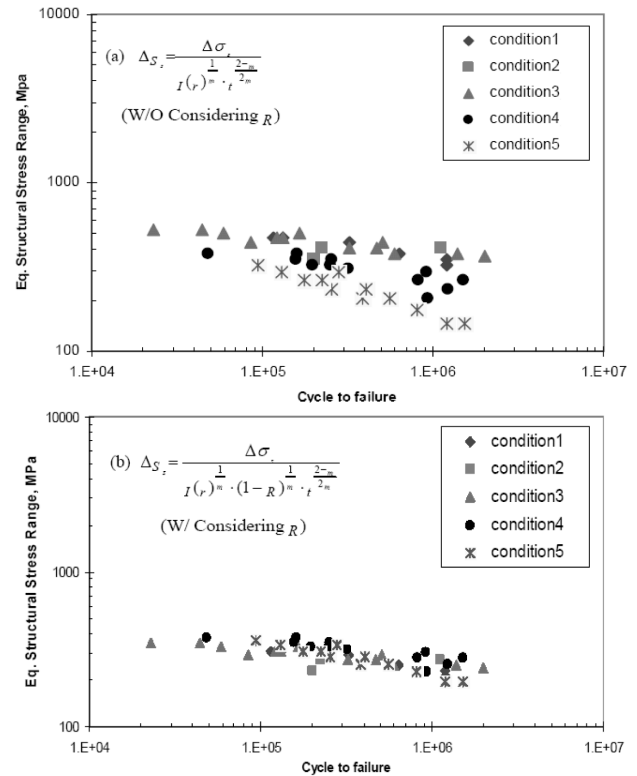


Fig. 8. Comparison of Equivalent Structural Stress Range Versus N with and Without Considering Loading Ratio R Effects

4. CONCLUSIONS

The major findings of the present study are as follows:

(1) A fatigue crack growth law considering high mean loading is proposed by using a structural stress and fracture mechanics approach. The proposed law is proven to be effective in unifying the so-called anomalous short crack growth data with those for long cracks even under high mean loading, resulting in the regression correlation parameter $R^2=0.98$

(2) The loading ratio R effects on the crack growth rate are much stronger when R is negative than when R is positive.

(3) The proposed crack growth law approach considering high mean loading can effectively be applied to consolidate S-N data including experimental data under high mean load conditions.

REFERENCES

- [1] ASME B&PV Committee, ASME B&PV Code Section III (2001).
- [2] Dong, P. Hong, J.K. and Cao, Z., "A New Mesh-

- Insensitive Procedure for Characterizing Stress Concentration at Welds," Proceedings of ASME PVP Conference, Vol.427, pp.22-26 (2001).
- [3] Sadananda, K and Vasudevan, A.K., "Short Crack growth Behavior," Fatigue and Fracture Mechanics: 27th Volume, ASTM STP 1296, pp.301-316 (1997).
 - [4] Kim, J.S., Jin, T.E., Hong, J.K. and Dong, P., "Finite Element Analysis and Development of Interim Consolidated S-N Curve for Fatigue Design of Welded Structure," Transactions of KSME A, Vol.27, No.5, pp.724-733 (2003).
 - [5] Kim, J.S. and Jin, T.E., "A Study on Fatigue Analysis Procedure of Nuclear Welded Structures Based on Structural Stress and Fracture Mechanics Approach," Proceedings of ASME PVP Conference, Vol.479, pp.49-55 (2004).
 - [6] Shin, C.S. and Smith, R.A., "Fatigue Crack Growth at Stress Concentrations-the Role of Notch Plasticity and Crack Closure," Engineering Fracture Mechanics, Vol.29, No.3, pp.301-315 (1988).
 - [7] Dong, P., Hong, J.K. and Cao, Z., "Stresses and Stress Intensities at Notches: Anomalous Crack Growth," International Journal of Fatigue, Vol.25, pp.811-825 (2003).
 - [8] Dong, P. and Hong, J.K., "A Two-stage Crack Growth Model Incorporating Environmental Effects," Proceedings of ASME PVP Conference, Vol.482, pp.104-113 (2004).
 - [9] Tada, H., Paris, P.C. and Irwin, G.R., "The Stress Analysis of Cracks Handbook," The Third Edition, ASME, New York, NY10006 (2000).
 - [10] Tanaka, K. and Nakai, Y., "Propagation and Non-Propagation of Short Fatigue Cracks at a Sharp Notch," Fatigue of Engineering Materials and Structures, Vol.6, No.4, pp.315-327 (1983).
 - [11] Sadananda, K. and Vasudevan, A.K., "Short Crack Growth Behavior," Fatigue and Fracture Mechanics: 27th Volume, ASTM STP 1296, Piascik, R.S., Newman, J.C. and Dowling, N.E., eds., pp.301-316 (1997).